Speckle Noise Suppression In SAR Images (Oil Spill Images) Using Wavelet Based Methods And ICA Technique

Bharaneswari.M
Research Scholar
School of Advanced Sciences
VIT University
Vellore. India
bharaneswari.m@vit.ac.in

Arulmozhivarman.P
Professor
School of Electronics Engineering
VIT University
Vellore. India
parulmozhivarman @vit.ac.in

Rao Tatavarti
Director (Research and Consultancy)
Gayatri Vidya Parishad Scientific and Industrial Research Centre
Visakhapatnam, India
rtatavarti@gmail.com

Senthilnathan.K
Associate Professor
School of Advanced Sciences
VIT University
Vellore. India
senthilnathan.k@vit.ac.in

Abstract — **Synthetic Aperture Radar (SAR) images are inherently degraded due to the coherent nature of the scattering phenomena called speckle. The presence of speckle decreases the utility of the SAR images by reducing the ability to detect ground objects. It affects the quality of the image adversely and hampers the observation of vital and crucial information present in the image. In this paper, we present an analysis of speckle suppression based on Wavelet decomposition methods. The algorithms viz., Projection Onto Approximation Coefficients (POAC), Projection Onto Span Algorithm (POSA) and Independent Component Analysis (ICA) are implemented on real SAR images and their results are tabulated. A comparison is made with standard speckle filters such as Lee filter, Frost filters, etc. The performance of our method is measured in terms of Peak Signal to Noise Ratio (PSNR) values.**

Keywords — ***SAR, Speckle, De-noise, Wavelet, PSNR***

I. INTRODUCTION

Synthetic Aperture Radar (SAR) is an active microwave remote sensing satellite or airplane, which has the capability to penetrate all clouds, haze and dark. It produces high spatial resolution imagery of Earth's land and sea surface in ultimately all-weather conditions, using special signal processing techniques. [1, 2]. However, the main disadvantage of the SAR images is the undesirable existence of the scattering phenomena, known as speckle[3]. Speckle gets introduced into the SAR image during acquisition stage or transmission stage of the radar signal[4]. The speckle appearing in synthetic aperture radar (SAR) images is generated by coherent interference of the radar echoes from the target scatters. Basically, speckle noise has the nature of a multiplicative noise[3], which causes a pixel-to-pixel variation in intensities and this variation manifests itself as a granular noise pattern in SAR images.[5,6].

Speckle noise degrades the appearance, reduces the image quality, complicates the human visual image interpretation and affects the effectiveness of image segmentation and feature classification process to a greater extent[5,6,7]. Hence, it needs to be suppressed efficiently, so as to retain the important features and to extract the underlying information from the images. Unfortunately 100% speckle removal is not possible. Therefore, a tradeoff has to be made among all these requirements.

II. SPECKLE DE-NOISING TECHNIQUES

Extensive research had been carried out to reduce the speckle noise from the SAR images for the past few decades, considering the speckle as the multiplicative as well as the additive noise in accordance to the speckle models and the domain. The main objectives of speckle de-noising are suppressing the speckle noise in uniform regions, preserving and enhancing edges without altering the important features and to provide a good visual appearance[8]. Speckle de-noising can be achieved mainly by two approaches, viz., Multi-look processing and Spatial domain filtering. By multi-look processing technique, multiple measurements of an object's (pixels) backscatter from different locations are considered and calculated. By spatial filtering technique, the average or median value of adjacent pixels are calculated to average out the speckle[15]. Many statistical filters are readily available for the speckle reduction, such as, Mean, Median, Box filter, Kuan filter, Lee filter, Frost filter, Enhanced Lee filter, Enhanced Frost filter and so on... The results show that statistical filters which are good at speckle reduction, lose important features. In recent years, there has been an active research on wavelet based speckle reduction as it provides multi-resolution decomposition and analysis of the image. In wavelet sub-bands, the presence of noise is mainly in the small coefficients and presence of important feature details are in large coefficients. So, once the small coefficients are removed, the resultant image will be noise-free. [9]. The three main steps involved in speckle de-noising in the wavelet domain are

(i) Applying Discrete Wavelet Transform (DWT) on the input image to decompose into 4 sub-bands namely LL (Approximation of the input image), LH (vertical details), HL (horizontal details), HH (diagonal details),

(ii) Manipulating the wavelet coefficients in the wavelet domain, which results in de-noising, and

(iii) Applying inverse wavelet transform (IDWT) to reconstruct the in the original domain.

III. METHODOLOGY

In this paper, we have considered various de-noising methods such as POAC[10], POSA[11], ICA[12,13] and compared with that of the Standard statistical filters such as Lee filter, Frost filter, etc. These methods are implemented to the original SAR image in the wavelet domain.

A. POAC

POAC[10] is a wavelet domain technique in which the image is decomposed into sub-bands using 2-D DWT. The sub-bands are LL, LH ,HL ,HH where L-represents low frequency components and H-represents high frequency components. The LL sub-band called as approximate coefficient containing most of the image information and very less noise while the other three sub-bands contains less image features and more noise. POAC can be analyzed by mathematical addition and projection of vectors. Now considering that noise is additive in nature, the coefficients of sub-bands HH, LH, HL can be expressed as the vector sum of image coefficient and noise coefficient. Therefore the vector 'y' for a noisy coefficient can be expressed as:

$$y = w\hat{} + n \quad (1)$$

where y = noisy coefficient of LH, HH, HL band

n = additive noise

$w\hat{}$ = coefficient of 'a' without noise.

The eqn.(1) can be expressed by the Figure.1 which explains the projection of y onto LL sub-band.

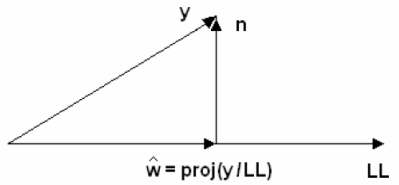

Fig.1 Vector diagram to represent POAC

Since we have to estimate *w*, we use an estimator which has been widely used for image restoration and reconstruction problems.

$$w = proj\,(\,y / LL) \quad (2)$$

where w is the projection of y onto LL where 'y' can be any of the noisy sub-bands. Therefore, *w* is mathematically expressed as,

$$w = \frac{trace(LL \cdot y^T)}{trace(LL \cdot LL^T)}\,\mathrm{LL}. \quad (3)$$

which gives three possibilities ,they are:

$$w_{LH} = S_{LH}\,.LL \quad (4)$$

$$w_{HL} = S_{HL}\,.LL \quad (5)$$

$$w_{HH} = S_{HH}\,.LL \quad (6)$$

where

$$S_{LH} = \frac{trace(LL \cdot LH^T)}{trace(LL \cdot LL^T)} \quad (7)$$

$$S_{HL} = \frac{trace(LL \cdot HL^T)}{trace(LL \cdot LL^T)} \quad (8)$$

$$S_{HH} = \frac{trace(LL \cdot HH^T)}{trace(LL \cdot LL^T)} \quad (9)$$

Hence, we generate three new scalars w_{LH}, w_{HL} and w_{HH} given by the equations 4,5,6, as a result of POAC, which are uncorrelated with respect to noisy sub-bands. These three scalars, along with the LL band can be used to perform IDWT to reconstruct the de-noised image.

B. POSA

We strat the techniue by decomposing the speckled SAR image into four wavelet subbands: Approximation coefficients (LL), and speckled coefficients of Horizontal Detail (LHs), Vertical Detail (HLs) and Diagonal Detail (HHs) respectively, as shown in Fig. 2, where: L represents Low frequency, H represents High frequency, DWT-2D means Bidimensional Discrete Wavelet Transform, and IDWT-2D means the inverse of DWT-2D.

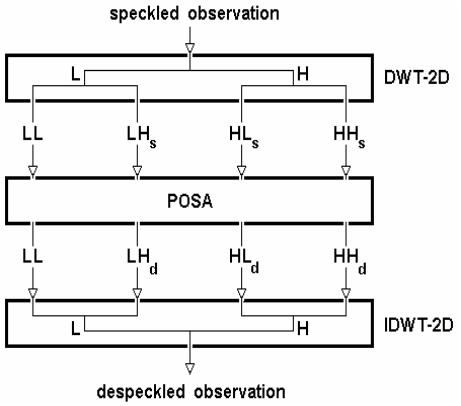

Fig.2 Projection onto Span Algorithm Representation

Let us suppose that, {LL, LHs , HLs , HHs} is a basis for an inner product space *W*. Let

$$\boldsymbol{LL} = LL / \|LL\|$$

$$\boldsymbol{LHs} = LHs / \| LHs \| \quad (10)$$

$$\boldsymbol{HLs} = HLs / \| HLs \|,$$

thus

$$LHd = \langle LHs , \boldsymbol{LL} \rangle \boldsymbol{LL}$$

$$HLd = \langle HLs , \boldsymbol{LL} \rangle \boldsymbol{LL} + \langle HLs , \boldsymbol{LHs} \rangle \boldsymbol{LHs}$$

$$HHd = \langle HHs , \boldsymbol{LL} \rangle \boldsymbol{LL} + \langle HHs , \boldsymbol{LHs} \rangle \boldsymbol{LHs} + \langle HHs , \boldsymbol{HLs} \rangle \boldsymbol{HLs} \quad (11)$$

where <A, B> represents the inner product of all real matrices A and B having the same number of columns, where <A, B> ≡ trace ($A\,B^T$). Finally, Equations (10) and (11) represents the POSA. The reconstructed image (here, the de-noised image) is the inverse of DWT-2D of the POSA output, as illustrated in Fig.2.

C. ICA

The ICA[12] is a well-established statistical signal processing technique which aims at decomposing a set of multi-variate signals into a base of statistically independent data-vectors with the minimal loss of information.

The linear equation which represents the ICA model can be written as

$$\begin{bmatrix} x_1(t) \\ x_2(t) \\ . \\ . \\ x_n(t) \end{bmatrix} = A \begin{bmatrix} s_1(t) \\ s_2(t) \\ . \\ . \\ s_n(t) \end{bmatrix} \quad (12)$$

where X is the observed vector of N samples ($x_1, x_2, \ldots\ldots x_n$), A is called the mixing matrix and S represents statistically independent components(IC's). It is assumed that the original signals are independent and almost all have non-Gaussian distributions. ICA model cannot be used if the individual components have Gaussian distributions. The basic task of ICA is to estimate A and S using only the observed vector X. The observed mixture is first pre-processed using centering and whitening where we make X as zero mean and unit variance respectively. In this paper we have used the Fast Fixed Point Algorithm [13,14] in order to find the mixing matrix. Once we find the mixing matrix, the independent components(IC's) can be found out easily as:

$$X = AS \Rightarrow S = A^{-1} X \quad (13)$$

From S, the required independent components are estimated.

As the SAR images may not be square images, two methods have been adopted in this paper. In the first method, the SAR image is resized into the nearest powers of 2 in the first method and then decomposed into the wavelet domain. In the second method, the original SAR image is resized into the next power of 2 by padding it with zeroes at the corners of the image before it is being decomposed into the wavelet domain. In both the cases, Wavelet decomposition performed is of level 1. Keeping in mind, the symmetry properties of wavelets and performance, the family of wavelets was chosen to be Daubechies (1-20), Coiflet (1-5) and Symlet (1-15).

A. First method (Non-Zeropadded SAR image de-noising)

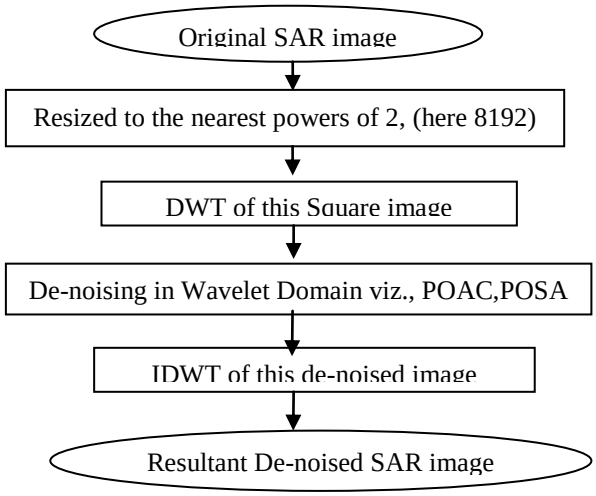

Flowchart.1 De-noising the Non-Zero-padded SAR image

Step-1: The SAR images are resized into the next highest powers of 2, here, 8192 pixels × 8192 pixels by linear interpolation. (Note: Cubic convolution cannot be used for original SAR images, as it yields negative results)

Step-2: DWT is applied on this resultant square image.

Step-3: Speckle de-noising method is applied on this DWT image / in the wavelet domain

Step-4: Take IDWT on this image

Step-5: This image after IDWT will have has the same 16-bit of the original SAR image and it is the de-noised result of the original SAR image and the results obtained are tabulated for different wavelet families.

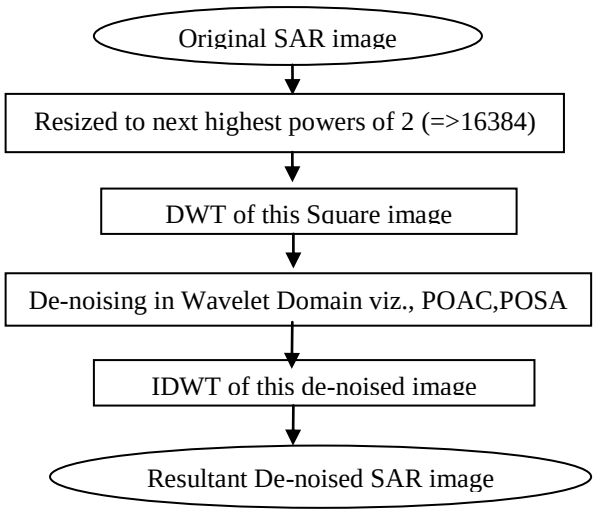

Flowchart.2 De-noising the Zero-padded SAR image

B. Second method:

Step-1: The SAR images are resized into the next highest powers of 2, here, 16384 pixels × 16384 pixels (i.e., padded with zeros) by linear interpolation.

Step-2: DWT is applied on this resultant square image.

Step-3: Speckle de-noising method is applied on this DWT image

Step-4: Take IDWT on this image

Step-5: This image after IDWT has the same 16 bit of the original SAR image and it is the de-noised result of the original SAR image. The performance of different de-noising methods is measured in terms of PSNR values and the results obtained are tabulated for different wavelet families.

IV. Experimental Results with Polarimetric SAR data:

The studies were carried out for two different SAR images of RADARSAT-2 Satellite in GEOTIFF format in 16-bit with different spatial resolutions, viz., one high resolution and one medium resolution obtained from National Remote Sensing Centre, Hyderabad.

The speckle de-noising methods such as POAC, POSA and ICA are applied to these SAR images in GEOTIFF format using ENVI software and called in IDL Programming language.

A. Study Area: Mumbai Oil spill region - 2010

The input SAR image is a RADARSAT-2, C-Band (5.3 GHz) image. It was taken on August 15, 2010 of Mumbai region, after the Oil spill on August 7th, 2010. The area covered in the image is 50km × 50km. The size/dimensions of the SAR image is 8802 pixels × 8476 pixels. The resolution is 9.5m (Near) and 8.8m (Far). The image is VV polarized, with an incident angle of 33.45˚ and beam mode MF22F (Multi-Look Fine Resolution Beam) with the Lat-Long centre at 18˚ 50' N and 72˚47' E.

B. Study Area: Mumbai Oil spill region - 2011

The input SAR image is a Radarsat-2, C-Band (5.3 GHz) image obtained from National Remote Sensing Centre, Hyderabad. It was taken on August 10, 2011 of Mumbai region, after the Oil spill from the night of August 6th to August 8th, 2011. The area covered in the image is 100km × 100km. The size/dimensions of the SAR image is 8766 pixels × 8243 pixels. The resolution is 27m (Near) and 22.7m (Far). The image is VV polarized, with an incident angle of 30.96˚ and beam mode S3 (Standard Beam) with the Lat-Long centre at 18˚44' N & 72˚38' E.

DE-NOISING OUTPUTS FOR SAR IMAGE -1(MUMBAI OIL SPILL 2010)

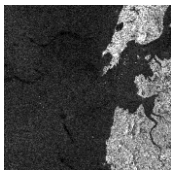
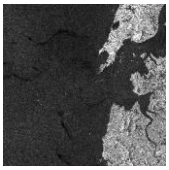
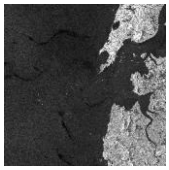

Fig.1 *Input image* Fig.2 *Lee* Fig.3 *Enhanced Lee*

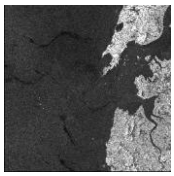
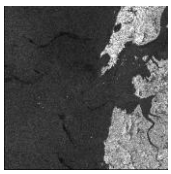
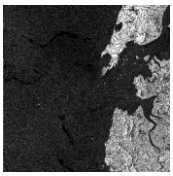

Fig.4 *Frost* Fig.5 *.Enhanced Frost* Fig.6 *POAC for db-1*

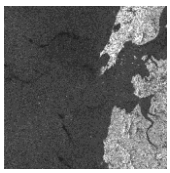
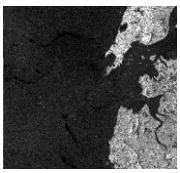
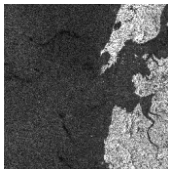

Fig.7 *POAC for Symlet-5* Fig.8 *POSA for db-1* Fig.9 *POSA for Coif-1*

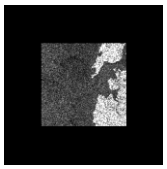
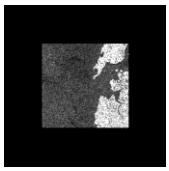
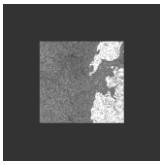

Fig.10 *Input Zero padded* Fig.11 *POAC for db-1* Fig.12 *POAC for db-4*

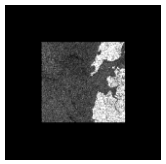
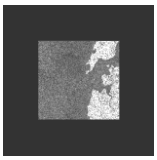
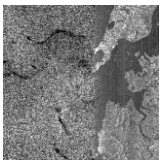

Fig.13 *POSA for db-1* Fig.14 *POSA for db-6* Fig.15 *ICA*

DE-NOISING OUTPUTS FOR SAR IMAGE-2 (MUMBAI OIL SPILL 2011)

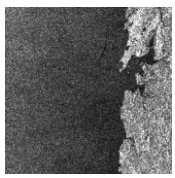

Fig.16 *Input image* Fig.17 *Lee* Fig.18 *Enhanced Lee*

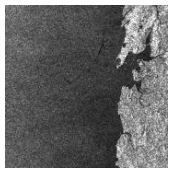
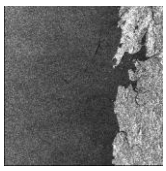
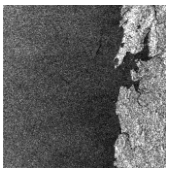

Fig.19. *Frost* Fig.20. *Enhanced Frost* Fig.21. *POAC for db-1*

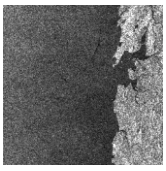
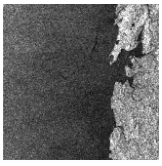
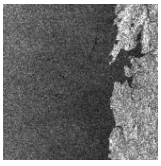

Fig.22. *POAC for Coif-3* Fig.23 *POSA for db-1* Fig.24 *POSA for Coif-3*

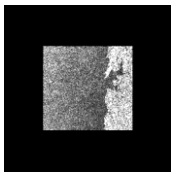
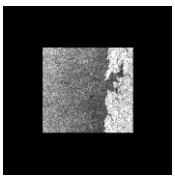
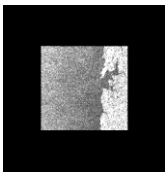

Fig.25. Input Z.pad Fig.26. *POAC for db-1* Fig.27. *POAC for Coif-2*

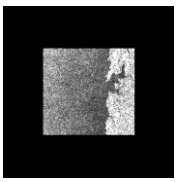
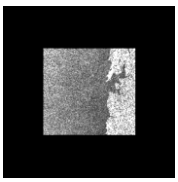
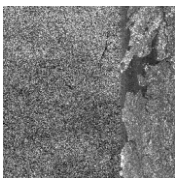

Fig.28 *POSA for db-1* Fig.29 *POSA for Coif-4* Fig.30. *ICA*

From the outputs shown in Fig.1-30, it is noticed that, ICA output has good contrast and brightness features for oil spill, while POAC and POSA smoothens better with preserving edges and textures when compared with all the other methods. It is observed that, in the wavelet family, db1 yields better PSNR values in both first and second methods. While the highest PSNR value is noticed for db1, the second and third highest values were also noted in the Table-1 below. When compared with other wavelets, the value obtained for db1 is found to be more than two times the value of second highest PSNR values.

TABLE I. DE-NOISING RESULTS

Filters / methods used for de-noising			Input SAR images	
			Mumbai 2010 with High resolution (More Oil Spill)	*Mumbai 2011 with Medium resolution (Less Oil Spill)*
Lee filter			27.6581	29.4442
Enhanced Lee filter			21.2323	23.2395
Frost filter			21.3249	23.3835
Enhanced Frost filter			21.3124	23.1766
POAC	Zero pad	1	48.3846 (db1)	51.1441 (db1)
		2	21.0157 (db4)	31.4386 (coif2)
		3	20.9965 (db17)	30.4245 (coif4)
	No Zero pad	1	44.5879 (db1)	46.4622 (db1)
		2	22.6668 (symlet5)	33.1111 (coif3)
		3	22.0881 (db4)	31.1046 (coif1)
POSA	Zero pad	1	48.3802 (db1)	51.1431 (db1)
		2	20.6474 (db6)	31.3930 (coif4)
		3	20.6185 (coif1)	28.3318 (symlet8)
	No Zero pad	1	44.5891 (db1)	46.4629 (db1)
		2	21.8505 (coif1)	32.7493 (coif3)
		3	21.8065 (db4)	31.0121 (db6)
ICA			30.1726	29.6536

V. CONCLUSION

In this paper, we have implemented various methods to de-noise the original SAR images in the remote sensing software ENVI (ver. 4.8) and IDL (8.0) successfully on HP Z400 Workstation, Intel Xeon Processor W3565 3.20 GHz, Quad-Core, 24 GB RAM.

Out of the best standard de-noising filters and other methods, viz., Lee filter, Frost Filter, POAC, POSA and ICA, a comparison is stated in this work. From the results obtained, it is noted that the wavelet based methods proved to be efficient in de-noising the original SAR images, which is measured in terms of the PSNR values. The results prove that our proposed technique shows better PSNR than all the standard filters used in remote sensing tools.

In the different family of wavelets, it is found that db1 outperforms all the other wavelets in this study, which is in plausible agreement with the other research outcomes in this field viz., [10] and [11]. In our results, it is observed that db-1 provides de-noised SAR images more than two times when compared to that of PSNR values of other wavelets.

Acknowledgment

Authors would like to acknowledge to the Defence Research and Development Organization, New Delhi, for sponsoring the research project at School of Electronics Engineering at VIT University. We also thank VIT University for providing necessary research facilities to carry out this research work.

References

[1] J. .Bruniquel and A.Lopes, "Multivariate optimal speckle reduction in SAR imagery," Int. Journal of Remote Sensing, vol. 18, pp. 603-627, Feb 1997.

[2] Saevarsson, B.B, Sveinsson, J.R, Benediktsson J.A, "Combined wavelet and curvelet denoising of SAR images", IEEE Trans. on Geosciences and Remote Sensing, Vol. 6, Sept 2004, pp.4235-4238.

[3] J.S.Lee, "Speckle suppression and analysis for Synthetic Aperture Radar images", Opt.Eng. 25(5), 255636, May 1, 1986.

[4] Milindkumar V.Sarode and Prashant R. Deshmukh, "Reduction of speckle noise and image enhancement of images using filtering technique", Int. Journal of Advancements in Technology, Vol.2, No.1, Jan 2011, pp.30-38.

[5] Jong-Sen Lee and Eric Pottier, Polarimetric Radar imaging from basics to applications, 1st ed., CRC Press, 2009, pp.101.

[6] J.S.Lee, I.Jurkevich, P.Dewaele, P.Wambacq, and A.Costerlinck,"Speckle filtering of synthetic aperture radar images: A review," Remote Sens. Rev., vol. 8, Apr. 1994, pp.311–340

[7] C.H.Chen and Xianju Wang, "A novel theory of SAR image restoration and Enhancement with ICA", IEEE Trans. on Geosciences and Remote Sensing, Vol. 6, Sept 2004, pp.3911-3914.

[8] A.Rajamani and V.Krishnaveni, " Performance analysis survey of various SAR image despeckling techniques", Int. Journal of Computer Applications, vol.90, No.7, March 2014, pp.5-17.

[9] Parthasarathy Subashini and Marimuthu Krishnaveni (2012). Image Denoising Based on Wavelet Analysis for Satellite Imagery, Advances in Wavelet Theory and Their Applications in Engineering, Physics and Technology, Dr. Dumitru Baleanu (Ed.), ISBN: 978-953-51-0494-0, InTech, DOI: 10.5772/36140. Available from: http://www.intechopen.com/books/advances-in-wavelet-theory-and-their-applications-in-engineering-physics-and-technology/image-denoising-based-on-wavelet-analysis-for-satellite-imagery.

[10] Mario Mastriani, "Denoising and compression in wavelet domain via Projection onto Approximation Coefficients", Int. Journal of Information and Communication Engineering, Vol. 5, No. 1, 2009, pp.20-30.

[11] Mario Mastriani, "New wavelet-based superresolution algorithm for speckle reduction in SAR images", World Academy of Science, Engineering and Technology, Vol.2, No.3, 2008, pp.850-857.

[12] Aapo Hyvärinen and Erkki Oja, "Independent Component Analysis: Algorithms and Applications", Neural Networks,Vol.13, 2000, pp.411-430.

[13] Aapo Hyvärinen and Erkki Oja, "A fast fixed-point algorithm for independent component analysis", Neural Computation,Vol.9, No.7, 1997, pp.1483-1492.

[14] A.Hyvarinen and E.Oja, "Fast and robust fixed-point algorithms for independent component analysis",IEEE trans on Neural networks,Vol.10, No.3, Nov.1999, pp.626-634.

[15] Bu-Chin Wang, Digital signal processing techniques and applications in Radar image processing, 1st Ed., 2008, pp.189.